JOURNAL OF GUIDANCE, CONTROL, AND DYNAMICS
Vol. 27, No. 6, November–December 2004

Transit-Orbit Search for Planar Restricted Three-Body Problems with Perturbations

Hideaki Yamato* and David B. Spencer†
The Pennsylvania State University, University Park, Pennsylvania 16802

A new class of trajectory search methods for the planar circular restricted three-body problem (CR3BP) with perturbations is presented. In the phase space of the CR3BP, there exist bundles of trajectories involving the transition from one region to another inside invariant manifolds of libration point orbits. Under the influence of perturbing forces, although these trajectory bundles can change their distributions and the locations, they still remain as orbit bundles for a considerable time in the phase space of the perturbed CR3BP. This paper presents a simple procedure of locating these orbit bundles directly in the CR3BP with perturbations. It is shown that by formulating the circular restricted problem of six bodies with the sun and the elliptical restricted problem of four bodies as perturbed CR3BP systems, the bundles of these solution orbits can be systematically and directly found on an arbitrarily chosen Poincaré section.

Nomenclature

D	=	distance between the larger and the smaller celestial bodies, DU
e, $\boldsymbol{e}$	=	orbital eccentricity and orbital eccentricity vector
J, ΔJ	=	Jacobi constant and change in Jacobi constant, DU^2/TU^2
L	=	libration point
R, r	=	distance between the celestial body and the spacecraft in rotating and pulsating frames, DU
t	=	time, TU
U^*, u	=	effective potential functions in rotating and pulsating frame coordinates, DU^2/TU^2
V_X, V_Y	=	X and Y direction velocity in rotating frame, distance units/time units (DU/TU)
X, Y	=	rotating frame coordinates, DU
${}^iX$, ${}^iY$	=	inertial frame coordinates, distance units (DU)
x, y	=	pulsating frame coordinates, DU
θ	=	position angle or true anomaly, deg
μ, η	=	normalized mass parameters for three-body and four-body systems
ϕ	=	angle between two eccentricity vectors, deg

Subscripts

G/E0	=	initial location of Ganymede relative to Europa
i, j	=	references libration points and celestial bodies
X, Y	=	partial derivatives with respect to X and Y

Introduction

THE phase-space geometry of the circular restricted three-body problem (CR3BP) has been researched by many authors.[1–5] An advantage in the use of the CR3BP for trajectory design or search problems is the availability of various solution orbits, which cannot appear in the two-body dynamics. As demonstrated by Barden,[1] Gómez and Masdemont,[2] and Howell et al.,[3] in addition to libration point orbits the existence of other invariant manifolds asymptotic to them can produce numerous trajectory options for space mission planning, including free transfers among the vicinity of the second-body and libration point orbits. The trajectory adopted for the Genesis space mission (launched in 2001 as part of NASA's Discovery Program) is the first example designed through the intensive analysis of the CR3BP manifold structure.[4,5]

As stated by several authors,[6–9] the inclusion of the third (and possibly the fourth) body as perturbations generally has a potential to reduce the required fuel consumption of transfers in terms of velocity change, compared with the classical two-body approach such as Hohmann transfers. In Belbruno and Miller,[6] for instance, the perturbation effect of the sun was explicitly considered in the transfer design from the Earth to the moon and produced the cost-effective transfers. In the design demonstrations, namely Shoot the Moon[7] and Petit Grand Tour,[8] the patched CR3BP approach was presented, where the restricted four-body system was decomposed into two CR3BP systems, and short orbital arcs found in these decomposed systems were patched together to yield entire transfers. It was shown that in both design concepts the resulting impulsive transfers featured large propellant mass reduction when compared with Hohmann-transfer cases.

Another application produced from the CR3BP phase-space analysis includes the study of cometary dynamics.[10,11] Based on the previous contributions by Conely[12] and McGehee[13] showing the existence of transit orbits and homoclinic orbits on libration point orbits, Koon et al.[11] presented heteroclinic connections between pairs of libration point orbits, providing an essential understanding of the transport mechanics. The dynamical phenomena observed in the solar system, such as the temporary capture of Helin-Roman-Crockett and the resonant transition of Oterma of the Jupiter family comets, have been intensively studied through the investigation of the sun/Jupiter CR3BP phase space.[10,11] In particular, the CR3BP model is used as a starting model to reproduce these comet trajectories available by the ephemeris data.

An outstanding geometric feature of the planar CR3BP phase space, shown by Koon et al.[7,8,11] and others,[12–14] is that invariant manifolds, formed by asymptotic solutions onto libration point orbits and appearing as deformed tubes in the phase space, remarkably enwrap all of the solution orbits passing from one region to another through libration points orbit. By taking full advantage of this feature, a procedure for the orbit construction with the prescribed sequence of transition regions was developed by Koon et al.[11] for the planar CR3BP system. In addition to the manifold trajectories on the tubular surface, the orbits inside the manifold tubes termed by transit orbits (e.g., orbits transiting from the exterior region to the region surrounding the second body or vice versa) are also

Received 12 August 2003; revision received 17 May 2004; accepted for publication 18 May 2004.

*Ph.D. Student, Department of Aerospace Engineering; currently Research Engineer, Future Robotics Technology Center, Chiba Institute of Technology, Chiba, 275-0016, Japan; yamato@furo.org. Member AIAA.

†Assistant Professor, Department of Aerospace Engineering; dbs9@psu.edu. Associate Fellow AIAA.

crucial in considering trajectory design applications. Using the Hill three-body problem, for instance, Villac and Scheeres[9] studied and characterized a wide rage of escaping trajectories from the second primary to the exterior regions through the $L2$ libration point orbits and provided some optimal criterion for that escaping.

The transit orbits, existing as trajectory bundles inside the manifold tubes of periodic orbits, can serve as transportation passageways in the CR3BP. The geometric structure of these passageways is an underlying mechanics of the transportation phenomena of comets and spacecrafts in the solar system. Lo and Ross[15,16] discussed the existence of a vast network of the transportation passageways originating from the invariant manifolds of libration point orbits in the CR3BP. The transportation network provides invaluable insights in understanding the transportation phenomena and in considering their applications to the trajectory design problem.

The primary objectives of this paper are to present a simple numerical procedure, for planar CR3BP systems with perturbations, of approximating these transportation passageways, consisting of solution orbits originally existing inside invariant manifolds of libration point orbits, and to show additional results of the existence of these passageways beyond the CR3BP. In the literature on transfer orbit design problems, a preestablished dynamical system consisting of several celestial bodies is decomposed into a series of CR3BP systems. Using the CR3BP as a starting model, a sequence of short orbital arcs are determined and numerically refined to gain the consistency with the original full-body system. The truncation of celestial bodies involved in the decomposition is required to simplify the design of short-orbit arcs. The methodology established in this paper can produce some facilitation in transfer design problems. Without using differential corrections, for instance, sets of impulsive orbit transfers within planar restricted problems of four bodies can be systematically found through the procedure presented here as shown in the subsequent work.[17]

In this paper, we first examine perturbation effects caused by the other bodies on bundles of transit orbits through numerical simulations. Based on the algorithm developed by Koon et al.,[7,8,11] an orbit search procedure is exploited, so that bundles of transit orbits can be found on the given Poincaré section in the planar CR3BP system under perturbations. The validity of the search procedure is evaluated by numerically simulating several dynamical systems, including the circular restricted four-body problem (CR4BP), the circular restricted six-body problem with the sun (CR6BPS), as well as the elliptical restricted four-body problem (ER4BP). Although the method is limited only to planar models, the method is featured by the uniform applicability to planar restricted three-body systems including several perturbation sources. In this paper, we use the Jovian system of Jupiter and Galilean satellites for the numerical demonstration, although the method can be used for the transit orbit search in other planar CR3BP systems with the perturbations.

Circular Restricted Three-Body Problem

Throughout the analysis in this paper, the dynamical system of the planar CR3BP is used as a nominal model. Before addressing the development of the design algorithm, the equations of motion for the planar CR3BP and a few basic features are briefly summarized here. For a detailed discussion of the CR3BP model, refer to Szebehely.[18]

Consider the motion of an infinitesimally small body in the gravitational field formed by two (larger and smaller) primaries. Assuming that two primaries are on circular orbits around their barycenter, the equations of motion for the third body in the rotating frame centered at the barycenter are expressed by

$$\ddot{X} - 2\dot{Y} = U_X^*, \qquad \ddot{Y} + 2\dot{X} = U_Y^*$$

$$U^*(X, Y) = (X^2 + Y^2)/2 + (1 - \mu)/R_1 + \mu/R_2$$

$$R_1 = [(X + \mu)^2 + Y^2]^{\frac{1}{2}}, \qquad R_2 = [(X - 1 + \mu)^2 + Y^2]^{\frac{1}{2}} \quad (1)$$

where X and Y, attached to U^*, represent the partial derivatives. The other normalized units, that is, the distance and the time units denoted by DU and TU, are defined as the distance between two primaries and the inverse of the angular velocity of the primary.

Table 1 Numerical constants used in simulation[19]

Gravitational source	GM, km^3/s^2	Mean distance, km
Jupiter	126,712,767.000	778,298,359
Europa	3,202.721	671,000
Ganymede	9,887.830	1,070,000
Io	5,959.915	422,000
Callisto	7,179.292	1,883,000

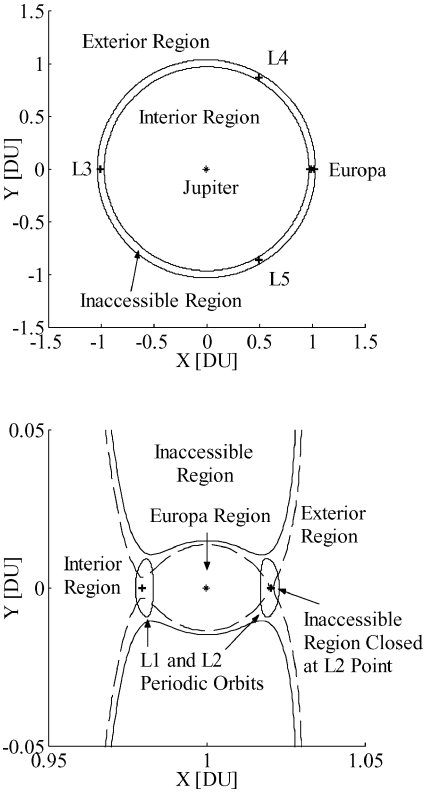

Fig. 1 Libration points, inaccessible region and $L1$ and $L2$ periodic orbits in the planar Jupiter–Europa CR3BP system.

Table 1 provides constants[19] used in this paper. The mean motion is obtained from the values in Table 1.

Normalized versions of these constants are used in the simulation. (The sum of the two masses is equal to one and the distance between the two masses is equal to one.) In the CR3BP phase space, there exist five equilibrium points called libration points. Following a widely used convention, these points are labeled Li, $i = 1 \sim 5$ as shown for the Jupiter–Europa system in Fig. 1. In addition to the libration points, the CR3BP has a constant of motion, named Jacobi integral, which is defined as

$$J = -(\dot{X}^2 + \dot{Y}^2) + 2U^*(X, Y) + \mu(1 - \mu) \quad (2)$$

In the design process, the Jacobi constant is a very useful tool to categorize a wide range of solution trajectories. In this paper, the Jacobi value given by Eq. (2) is used as an indicator of perturbation effects in the investigation of four-body systems approximated by the CR3BP (although there are no constants of motion for the perturbed CR3BP). Another feature of the CR3BP is the existence of periodic orbits around collinear libration points. These special solutions can be located by a systematic manner for various values of the Jacobi constant. The discussion about their determination is found in Howell.[20]

For each value of the Jacobi integral, there exists an inaccessible area, where the third body is not allowed to enter with the initial Jacobi constant J_0. The inaccessible region with some Jacobi constant slightly less than $J(L2)$ is depicted by the solid curve in Fig. 1. Note that the inaccessible region divides the area where the third

body can move into three regions. In this paper, we refer to these regions as the interior, exterior, and the second primary regions. As also shown by the dashed curve, the inaccessible region closes at the $L2$ point when the Jacobi constant is greater than $J(L2)$. Hence, it is infeasible for spacecraft to transfer from the interior or the exterior region to the smaller primary region. The trajectories with the Jacobi integral slightly less than $J(L2)$ are the main focus of this paper.

Phase-Space Structure of CR3BP

A comprehensive study on the phase-space geometry of the planar CR3BP was given by Koon et al.[11] We briefly summarize several important features including invariant manifolds of libration point orbits.

Manifold Structure

Associated with the $L1$ and $L2$ periodic orbits, there exist unstable and stable invariant manifolds in the CR3BP phase space. These invariant manifolds can be defined based on the hyperbolic feature of periodic orbits. In this paper, an invariant manifold of a libration point orbit is simply referred to as an invariant hypersurface in the phase space, formed by continuously distributed solution orbits asymptotic to the periodic orbit. Although there are other invariant manifolds, such as equilibrium points or periodic orbits, we use the term invariant manifolds only for those asymptotic to the periodic orbits for a distinction. Wiggins[21] and Perko[22] include additional mathematical descriptions about invariant manifolds for general dynamical systems.

Typical global and local structures of unstable and stable manifolds in the phase space (originally presented in Ref. 11) are visualized in Fig. 2 for the Jupiter–Europa planar CR3BP system. The collection of the black or gray curves indicates unstable or stable manifold, respectively, and the two distorted ellipses existing at the intersection of the manifolds in the local figure are the $L1$ and $L2$ periodic orbits. Although the projection of the manifolds onto the configuration space is shown, these manifolds have shapes of squashed and distorted tubes in the phase space. For the latter reference, the Poincaré section at $\theta = 180$ deg, defined by $X = 0$ and $Y < 0$ and labeled PS_{180}, is also illustrated by a solid line in the global figure, where the position angle θ is defined as the counterclockwise angle from the positive X axis. In the subsequent analysis, solution orbits crossing that section transversally are studied with the stable manifold in the exterior region.

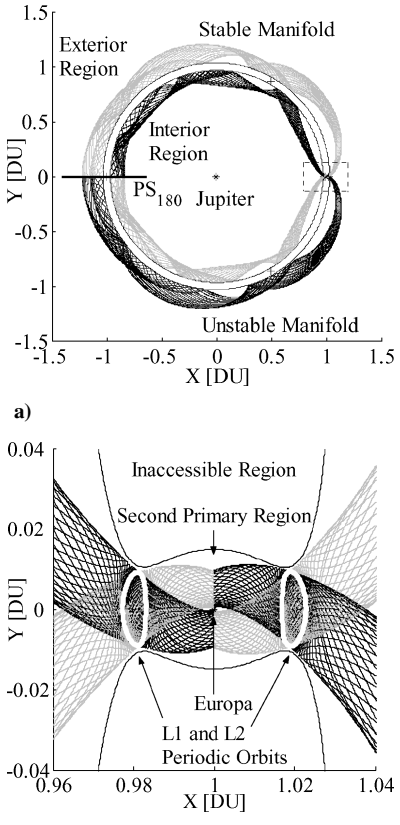

Fig. 2 Views of invariant manifolds of periodic orbits[11]: a) global and b) local.

Computing Method of Invariant Manifolds of Libration Point Orbits

The numerical method of computing manifolds is briefly described here. The method presented in Parker and Chua[23] is employed (also refer to Barden[1] and Howell[3]). After determining an $L1$ or $L2$ periodic orbit,[20] the following procedure is used to compute an unstable (or stable) manifold:

1) Find a set of initial values along the periodic orbit for the unstable (or stable) manifold using unstable (or stable) eigenvector of the monodromy matrix.

2) Integrate the CR3BP model from these initial conditions forward or backward in time until the third body reaches the given Poincaré section.

An important mathematical concept for the stability analysis of periodic orbits is called a monodromy operator (provided by Floquet theory[24]). The monodromy operator is the state transition matrix for one revolution along the libration point orbit in our case.[3] Using the unstable (or stable) eigenvector of the monodromy operator (or matrix), an initial value of an unstable (or stable) asymptotic solution can be approximated by slightly shifting a state on the periodic orbit in the direction of the unstable (or stable) eigenvector (it suffices to give 50-km offset along the eigenvector for the Jupiter/Galilean Satellite CR3BP system). By repeating this process along the periodic orbit, a set of initial values used for the manifold computation can be found. Numerical integrations of the CR3BP from these initial values generate a family of approximated asymptotic solution trajectories that form an invariant manifold tube in the phase space. For numerical integration in this paper, we used the fourth-order one-step explicit numerical integrator (ode45 in MATLAB®) with the relative and the absolute error tolerances of 10^{-10} and 10^{-12}, respectively.

Orbital Classification

A remarkable feature in the CR3BP phase space is the classification of solution orbits near the $L1$ and $L2$ libration points (called orbital classification for convenience). The orbital classification guarantees that solution trajectories, which pass by the $L1$ or $L2$ libration points, are classified into four types of orbits.[11] These four types of trajectories are schematically illustrated in Fig. 3. The first and second types are periodic orbits and trajectories asymptotic to them. The third type of trajectory is an orbit that transits from one region to another, for example, from the exterior region to the second primary realm in Fig. 3. Finally, the last type of orbit is a nontransit orbit, which remains in the same domain (the exterior, the interior, or the second primary region).

Another feature of the CR3BP phase space important for understanding its transport mechanics is that all of the solution trajectories inside the manifold tubes are transit orbits. Conversely, for the given

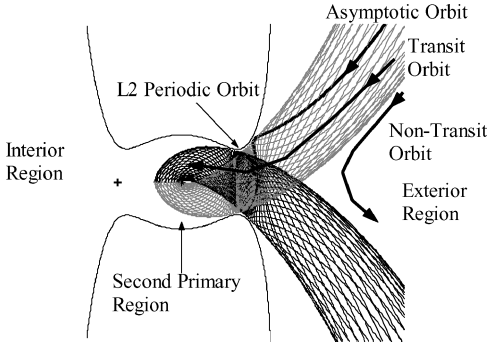

Fig. 3 Four types of solution trajectories near a libration point.[11]

value of the Jacobi integral, trajectories from one region to another exist only inside the manifold tube. From this sense, the manifold tube can be viewed as an enclosure of the transit orbit bundle. Gómez et al.[25] showed that the invariant manifold of libration point orbits can also act as separatrix in the phase space of the spatial CR3BP.

The practical importance of the orbital classification is in considering trajectory design problems. To achieve an encounter with the smaller primary effectively, for example, the first requirement is simply to enter the region of the smaller primary through the $L1$ or $L2$ periodic orbit. In Fig. 3, thus, the spacecraft must be inside the exterior stable manifold tube. The actual procedure to find such a trajectory can be greatly reduced. As demonstrated by Koon et al.,[7,8,11] in fact, a set of initial states resulting in transit orbits is systematically found on any Poincaré section for the ideal planar CR3BP. Thus, the main objective is to establish a methodology of finding transit orbits even with the presence of perturbations.

Transit-Orbit Search

In this section, we first demonstrate a numerical procedure[7,8,11] of finding transit orbits on an ideal planar CR3BP. Through numerical investigations on a planar three-body system with a fourth-body perturbation, we discuss the effectiveness and the limitation of that search procedure.

Transit-Orbit Search for Ideal CR3BP

To demonstrate the search procedure of transit orbits, a simple numerical simulation is performed on the ideal planar CR3BP, consisting of Jupiter, Europa, and the spacecraft without any perturbations. Consider the $L2$ exterior stable manifold tube and the Poincaré section at $\theta = 180$ deg in Fig. 2. The projection of their intersection on the X–V_X plane is shown in Fig. 4. Note that the intersection between the manifold tube and the Poincaré section is referred to as a manifold cut for convenience in this paper, and typically its projection on the X–V_X plane is used for the analysis. In Fig. 4, the left-side portion, represented by the dotted square box and corresponding to the outermost part from Jupiter, is enlarged. Although it is hard to see, the manifold cut appears as a highly squashed and distorted closed curve.

The objective is to identify a set of initial values on this Poincaré section, which are going to enter the region around Europa. The selection of initial values follows the procedure here:

1) Specify an initial location of the spacecraft in the configuration space by selecting X.

2) Choose values of the X-direction velocity inside the closed curve obtained by projecting the manifold cut on the X–V_X plane (Fig. 4).

3) Compute magnitudes of the Y-direction velocity from the Jacobi constant.

Because the Poincaré section is chosen as $X < 0$ and $Y = 0$, the selection of the value X can completely specify the physical location of the spacecraft. By referring to the manifold cut (X–V_X plot), it is possible to select the X-direction velocity inside the closed curve arbitrarily. It is then straightforward to compute the Y-direction velocity from the Jacobi constant for the planar CR3BP. (Note that for the spatial CR3BP this process might not be straightforward because of additional degrees of freedom.) Although Cartesian coordinates are used in the preceding list for simplicity, polar coordinates should be used in computer codes because the procedure can be applied at any angle of the Poincaré section.

For illustration, nine magnitudes of the X velocity, marked by the circles and the "x" for inside and outside values respectively, are arbitrarily selected for the initial location, $X = -1.227$ DU and $Y = 0$ DU. According to the orbital classification, if an initial state is inside the manifold cut, represented by the circles, the solution trajectory must be classified into the transit orbit, that is, it is guaranteed to enter the Europa region. For an initial state located outside the manifold cut, represented by the x, the solution trajectory cannot enter the Europa region. The CR3BP model is numerically integrated from the values selected, and the solutions are plotted in Fig. 5. As we expect, all of the trajectories emanating from the inside of the manifold cut can make the close encounter with Europa.

Through the search procedure in the preceding list, any points inside the manifold cut can produce transit orbits, allowing the generation of various trajectories involving the transition to the second primary region. In general, the high sensitivity caused by the inverse-square gravity field makes the search of a specific type of orbits very

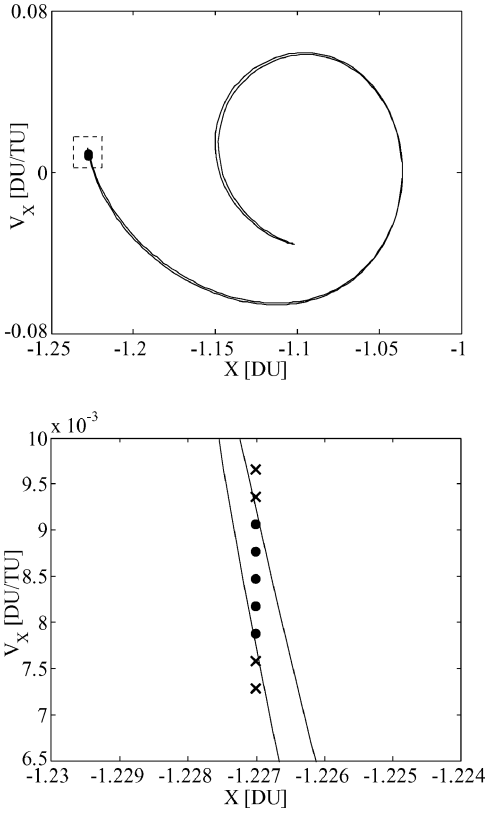

Fig. 4 Initial value selections in the CR3BP.

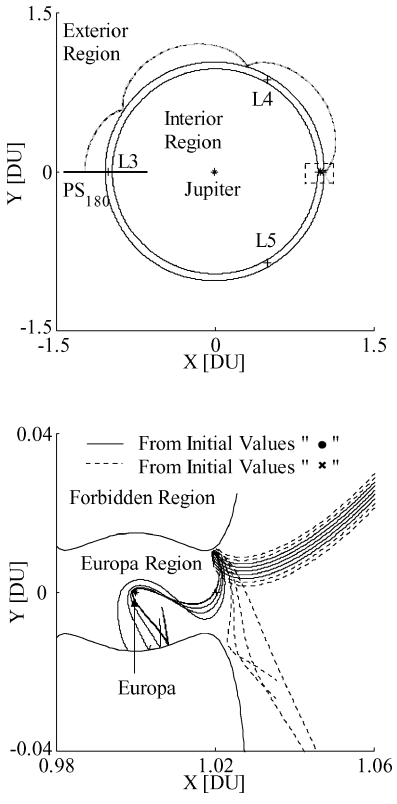

Fig. 5 Transit orbits in the CR3BP.

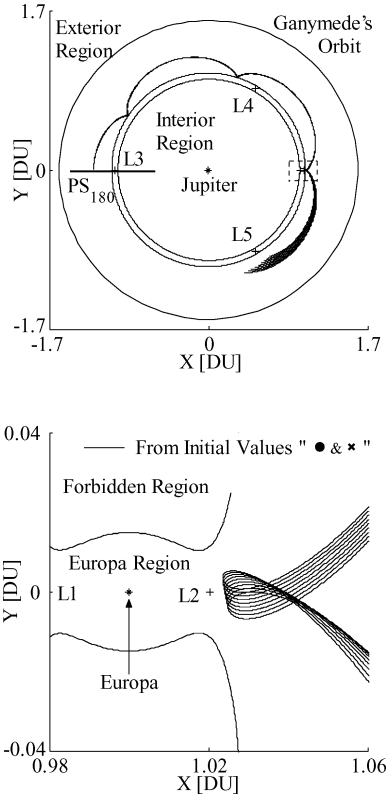

Fig. 6 Failure of transit orbit search in the CR3BP with perturbing body.

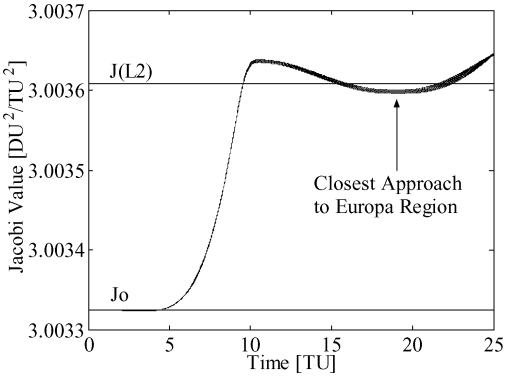

Fig. 7a Jacobi values along solution trajectories in the CR4BP.

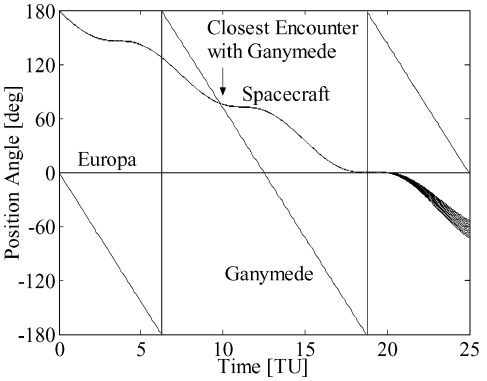

Fig. 7b Position angles of Europa, Ganymede, and spacecraft.

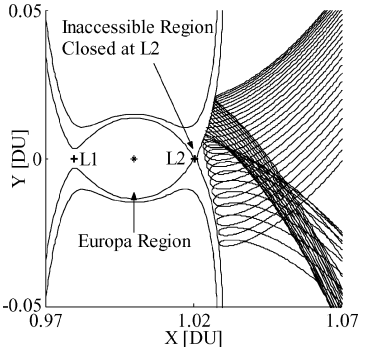

Fig. 8 Inaccessible region closed at *L*2 point.

challenging. The analysis of the manifold structure can, however, offer an excellent framework for constructing a spacecraft orbit.

Perturbation Effects on Orbital Structure

To observe the effects of perturbations on the procedure in the preceding list, the perturbed CR3BP model is numerically integrated with the exact same initial values as used in the preceding ideal case. The perturbed CR3BP used for this simulation consists of Jupiter, Europa, Ganymede, and the spacecraft. Ganymede is assumed to be on a circular orbit around the barycenter of the Jupiter–Europa system. The initial angle of Ganymede relative to Europa is arbitrarily selected as $\theta_{G/E0} = 0$ deg, that is, all of the bodies are initially aligned on the X axis. The solution trajectories generated by numerical integrations are plotted in Fig. 6.

With the presence of the perturbing body, all of the trajectories fail to enter the Europa region. Recall that five initial values, represented by circles in Fig. 4, were selected so that they were inside the stable manifold tube, and in fact, the trajectories starting with those values could all enter the Europa region. Note that Ganymede is orbiting around Jupiter on the far side of Europa when the spacecraft is making the close approach to the Europa region. Although not discussed here, it can be shown that in another initial configuration of Ganymede all of the initial states including the outside values provide transit orbits. The failure of this example implies that the search procedure in the preceding list is effective only for the ideal CR3BP.

Explanation of the Failure of Search Procedure

Before addressing the development of the design algorithm, it is worth considering the mechanics of the failure. One possible explanation is given by observing the Jacobi value in Eq. (2) along solution trajectories. In Fig. 7a, the Jacobi values along these solution orbits are plotted with respect to the canonical time. All of the Jacobi values start with the same value J_0, where J_0 indicates the Jacobi value on the associated $L2$ periodic orbit. Notice that they are approximately constant before $t = 5$ TU and at $t = 19$ TU. This implies that for those time periods the motion of the spacecraft in the four-body system can be modeled by the three-body dynamics, that is, the influence of the fourth body is negligible. However, the Jacobi values rapidly increase after $t = 5$ TU. During this period, the gravitational effect of the perturbing body (Ganymede) becomes much larger than Europa. In fact, Ganymede approaches and moves by the space vehicle around $t = 10$ TU, as indicated in Fig. 7b.

The closest encounter with Ganymede increases the Jacobi value in this numerical simulation. As a consequence, when the spacecraft makes the closest approach to Europa at $t = 19$ TU, all of the Jacobi values are roughly the same as the value at the $L2$ libration point, that is, $J(t = 19)\ J(L2)$. Recall that if the Jacobi constant has a value greater than $J(L2)$, the forbidden region closes at the $L2$ point as shown in Fig. 8, where the solution orbits with various X-direction velocities on the Poincaré section are replotted.

In Fig. 8, however, all of the trajectories still have a tendency to approach Europa. Furthermore, the changes in the Jacobi values caused by the perturbation in Fig. 7a are very similar among the trajectories starting from the fixed initial configuration. These observations are important in considering an alternative procedure for finding initial states of transit orbits. In this specific simulation, for instance, the Jacobi value increases roughly by $\Delta J \approx 0.0003$ as seen in Fig. 7a. Consider the case in which the space vehicle starts its transfer with a much smaller value, such as $J_{\text{adjusted}} = J_0 - \Delta J$. Even after the increase of the Jacobi value as a result of the encounter

with Ganymede, the spacecraft can still have an appropriate value, where the forbidden region can open enough when making the closest approach to the region of the second primary. In this case, there is a strong likelihood that the space vehicle would enter the smaller primary region. With this rough idea, we establish a new strategy of finding transit orbits.

Transit-Orbit Search for Perturbed CR3BP

The objective here is to establish a new strategy of locating initial values on an arbitrarily chosen Poincaré section, so that the spacecraft with these initial states is going to enter the smaller primary region including the presence of perturbing forces. This section presents an approach to the transit orbit search in perturbed CR3BP systems. The detailed description of the procedure including its application to planar impulsive transfer design is also found in Refs. 17 and 26.

Transportation Tubes in Perturbed CR3BP

The strategy for developing the algorithm is to numerically approximate the location of transit orbit bundles in the perturbed CR3BP. Thus, we assume that solution orbits, originally existing inside the manifold tube, still exist as bundles inside some deformed tube under perturbations, serving as a transportation passageway. The approximation of such a transportation tube is generated by a similar manner to the manifold computation. After determining a Lyapunov orbit without perturbations, we use the following steps to obtain a transportation tube:

1) Find a set of initial values used for the manifold computation by the same method for the CR3BP.

2) Numerically integrate the full dynamical model including perturbations from the initial states determined in the step 1 until the spacecraft reaches the given Poincaré section.

The same set of initial conditions as the manifold tube computation are used and propagated by numerically integrating the full model including perturbations. Recall that unstable and stable manifold tubes are generated by integrating the CR3BP model as summarized in the procedure in the phase-space structure of CR3BP section. The only difference is the use of the full dynamical model for the numerical globalization. Note that the procedure in the preceding steps is applicable to numerous perturbation sources and yields invariant manifolds of libration point orbits for the case that no perturbations exist.

Also note that unstable and stable manifolds of libration point orbits in the CR3BP are precisely defined in mathematical terms based on the existence and the hyperbolic feature of the periodic orbits,[21–23] that is, the existence of unstable and stable asymptotic solutions. Because the existence of periodic orbits is not guaranteed for the model including perturbations, we cannot expect that time-invariant manifolds exist for the perturbed system. Thus, the transportation tube introduced in the preceding steps is merely an alternative to locate transit-orbit bundles. However, the transportation tube can produce various benefits, including the systematic determination of transit orbit bundles. We use the term transportation tube only as a product computed by the preceding steps in order to distinguish it from invariant manifolds of libration point orbits obtained by the procedure listed in the phase-space structure section.

Visualization of Perturbation Effects

One of the motivations for introducing transportation tubes is that they can offer a practical means to visualize time-dependant effects of perturbations. In Fig. 9, similar to the manifold tube of the CR3BP, the cuts of several transportation tubes, that is, the intersection between the transportation tube and the Poincaré section ($\theta = 180$ deg), for the CR3BP with the fourth-body perturbation are projected on the X–V_X plane. The dotted and solid closed curves represent the cuts of the transportation and the manifold tubes, respectively. Note that the perturbation effect of the fourth body, Ganymede, depends on its initial location with respect to the second primary, Europa, as indicated by $\theta_{G/E0}$.

The global shapes of the transportation tubes are very similar to the shape of the manifold tube. If a small portion (represented by the dotted square box) is enlarged, however, it can be seen that the transportation tubes vary from the original location. We expect that the velocity magnitude required for the spacecraft to enter the smaller body region is much different among the initial configuration of the perturbing body.

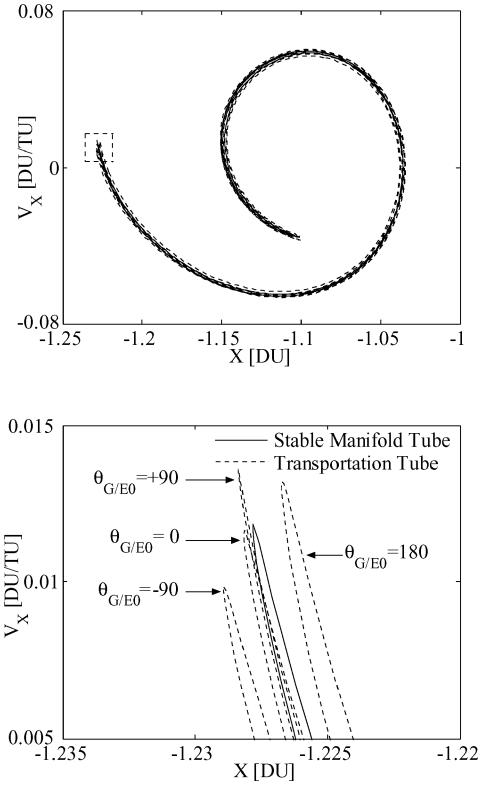

Fig. 9 Comparison between transportation and manifold tube cuts.

Adjustment of Jacobi Value

Another benefit of computing the transportation tube is that the cut of the transportation tube can be used for estimating an appropriate amount of the Jacobi value adjustment. The observation made earlier is the uniformity of the variation of the Jacobi value as seen in the failure example in Fig. 7a. The information on the appropriate adjustment is gained from the Jacobi value computed along the transportation tube cut. An example of the Jacobi value obtained along the transportation tube cut is shown in Fig. 10.

The closed curve represents the Jacobi value for the CR3BP with the fourth-body perturbation, and the black line labeled J_0 indicates the Jacobi constant for the ideal CR3BP system. As is clear from the figure, the Jacobi value for the four-body system varies from the original value as a result of the presence of the perturbing force. For each location of X, there are upper and lower bounds of possible Jacobi values. In this paper, a simple average

$$J_{\text{average}} = (J_{\text{upper}} + J_{\text{lower}})/2 \tag{3}$$

is used for the transit-orbit search. The effectiveness of this simple approximation will be evaluated by numerical simulation.

Augmented Search Procedure of Transit Orbits for Perturbed CR3BP

The augmented procedure for selecting initial values of transit orbits follows the process shown in the following steps. The process is the same as the normal selection procedure in the section on transit-orbit search for ideal CR3BP, except for the use of the transportation tube generated by the steps listed in the transportation tubes in perturbed CR3BP section and the adjusted Jacobi value computed by Eq. (3). In computer codes, the search procedure in the following steps can be automatically reduced to the normal procedure in the transit-orbit search for ideal CR3BP section if no perturbations exist. Similar to the preceding section, the case of the Poincaré section

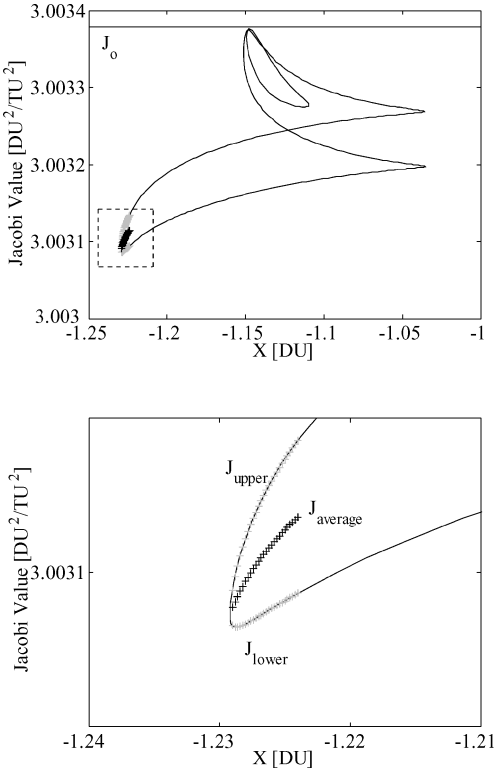

Fig. 10 Jacobi value along intersection between transportation tube and Poincaré section for the perturbed CR3BP.

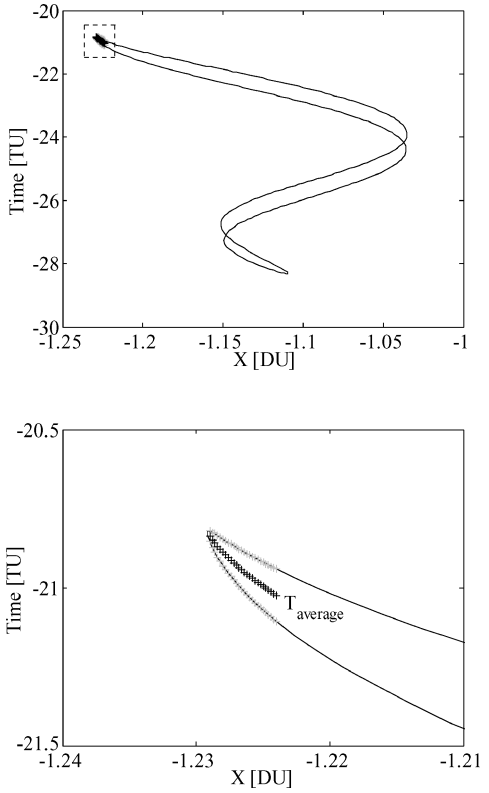

Fig. 11 Flight-time estimation.

at $\theta = 180$ deg with Cartesian coordinates is shown for simplicity. Note that the new procedure can be applied to various sources of perturbations, as is the computation of the transportation tube.

1) Compute the transportation tube cut by the steps of the procedure in transportation tubes in perturbed CR3BP section.

2) Choose an initial location of the spacecraft in the position space by selecting X.

3) Find an adjustment of the Jacobi value for the location selected in the step 2.

4) Specify a value of the X-direction velocity inside the transportation tube cut by referring to the X–V_X plot.

5) Compute the magnitude of the Y-direction velocity from the adjusted Jacobi value determined in the step 3.

Flight-Time Estimation

We can obtain the approximated flight time from the computation of the transportation tube. The flight time between the vicinity of the libration point and the Poincaré section at $\theta = 180$ deg is plotted against the X position on the Poincaré section in Fig. 11, where the left-side portion indicated by the dotted square box is enlarged. Note that the flight time is represented by negative values because the stable transportation tube is computed in reverse time from the vicinity of the periodic orbit.

The flight time depends on the location of X on the Poincaré section. We can estimate the flight time for transit orbits in a similar manner to the Jacobi value adjustment. For each location of X, the upper and the lower values are first determined, and the average of those values is adopted. For instance, approximately 21 TUs are necessary to reach the vicinity of the second primary realm for the spacecraft starting from $X = -1.225$ DU and $Y = 0$ DU.

Evaluations

We now evaluate the procedure of searching transit orbits in the preceding steps by numerically simulating the planar circular restricted four-body problem (CR4BP). To examine the applicability to other perturbed systems, we then apply the procedure to the planar circular restricted six-body problem with the sun (CR6BPS).

Transit-Orbit Search in Planar CR4BP

The augmented procedure in the preceding steps is applied to a planar CR4BP, consisting of Jupiter, Europa, Ganymede, and spacecraft. The CR4BP is modeled assuming that both moons are on concentric circular orbits around Jupiter in the same orbital plane. The dynamical model in the inertial frame with the origin at Jupiter is transformed to the model in the rotating frame at the same origin and rotating with Europa. The discrepancies of the CR4BP from the nominal CR3BP, caused by the additional body and the difference of the rotational center, are considered as perturbations. For the transportation tube computation, the initial angle of Ganymede with respect to Europa is arbitrarily chosen as $\theta_{G/E} = 0$ deg.

After constructing the exterior stable transportation tube, a number of initial states on the Poincaré section at $\theta = 180$ deg are selected between $X = -1.224$ DU and $X = -1.229$ DU by the steps of the procedure listed in the section on the augmented search procedure of transit orbit for perturbed CR3BP. The CR4BP is numerically integrated from those values. Note that the initial position angle of Ganymede when the spacecraft is on the Poincaré section is determined for each X location based on the estimated flight time.

The results of the numerical simulations are summarized in Fig. 12. The solid and dotted closed curves represent the cuts of the transportation and manifold tubes, respectively, and the left side is enlarged. Each black dot indicates an initial state resulting in a transit orbit. The numerical simulation shows that the solution trajectories starting from all of the black dots (more than 330) inside the transportation tube can enter the Europa region. This result leads to the conclusion that the transportation tube approximates the bundle of transit orbits quite well. Note that we apply the transit-orbit search only on the specific portion, corresponding to the farthest part from Jupiter, in this numerical evaluation.

Solution trajectories starting from $X = -1.227$ DU and $Y = 0$ DU with various velocity magnitudes are shown in Fig. 13, with the Jacobi values along those solution trajectories. Most of the example trajectories collide with Europa after entering the smaller primary region. For the transfer design problem, the crash into the second primary can be easily avoided by adjusting the X velocity. For any location on the Poincaré section, there is a permissible range for the X velocity selection as shown in Fig. 12. To find

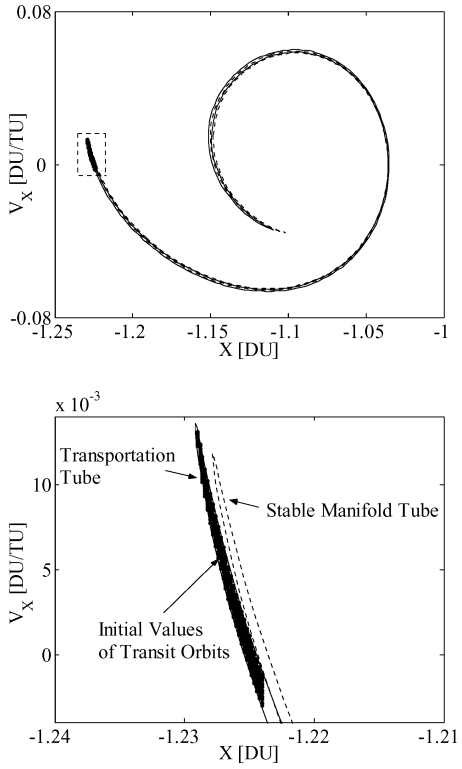

Fig. 12 Evaluation of the augmented search procedure in the CR4BP.

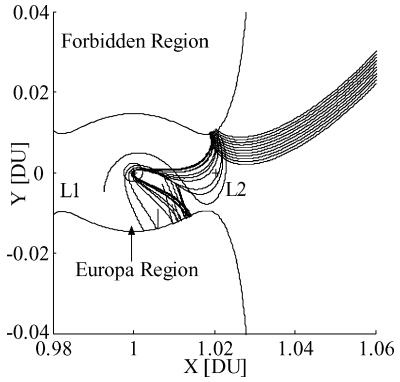

Fig. 13a Transit orbits in the CR4BP.

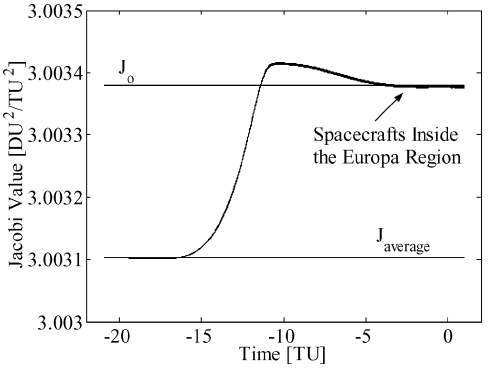

Fig. 13b Jacobi values along solution trajectories.

an orbit with specific properties, some targeting techniques, such as differential corrections, can be applied on the set of the transit orbits found through the procedure. In Fig. 13b, the value of the Jacobi constant on the approaching phase is approximately same as the original value, J_0, where J_0 is the value on the $L2$ periodic orbit in the case that no perturbations exit. This implies that the Jacobi value when the spacecraft is on the Poincaré section is suitably adjusted.

Transit-Orbit Search in Planar CR6BPS

The augmented procedure can also offer a practical means to find transit orbits in planar circular restricted problems of multiple bodies, where all of the celestial bodies are assumed on the circular orbits in the same orbital plane. To support this claim, we perform additional numerical simulations on a more realistic system: the planar circular restricted six-body problem with the sun (CR6BPS). In the planar CR6BPS, two more Galilean satellites, Io and Callisto, are added as perturbing bodies to the Jupiter/Europa/Ganymede CR4BP. Additionally, terms representing the gravitational force of the sun and the circulation of the Jovian system around the sun are included. The equations of motion for the CR6BPS are derived by applying the unit normalization and the coordinate transformation on the inertial frame model. For the transportation tube computation, the initial angles of all of the moons are impractically selected as $\theta = 180$ deg, and the initial location of the Jovian system with respect to the sun is arbitrarily selected as $\theta = 0$ deg. Thus, all of the perturbation sources of gravitations are initially located in the left side of the spacecraft.

The search procedure in the preceding steps is performed on the Poincaré section at $\theta = 180$ deg to find transit orbits toward the Europa region. The result of the numerical simulations is shown in Fig. 14. Similar to the CR4BP case, each transit orbit found through the procedure is represented by a black dot. In this evaluation, we apply the search procedure onto the entire domain inside the closed curve of the transportation tube cut. The transit orbits are uniformly found inside the transportation tube cut. The augmented search procedure is also effective for the planar CR3BP system under the influence of multiple perturbation bodies.

To evaluate the applicability to other perturbed CR3BP systems, the transit-orbit search is performed on the sun–Earth/moon CR3BP system with a perturbing-body Jupiter. In this model, the Earth and its moon are viewed as one mass circulating around the sun, and Jupiter is included as a perturbing body. The physical constants used for this simulation are taken from Ref. 19. The result of the transit orbit search is shown in Fig. 15. We can see from the figure that the procedure in the preceding steps can find transit orbits uniformly inside the transportation tube cut.

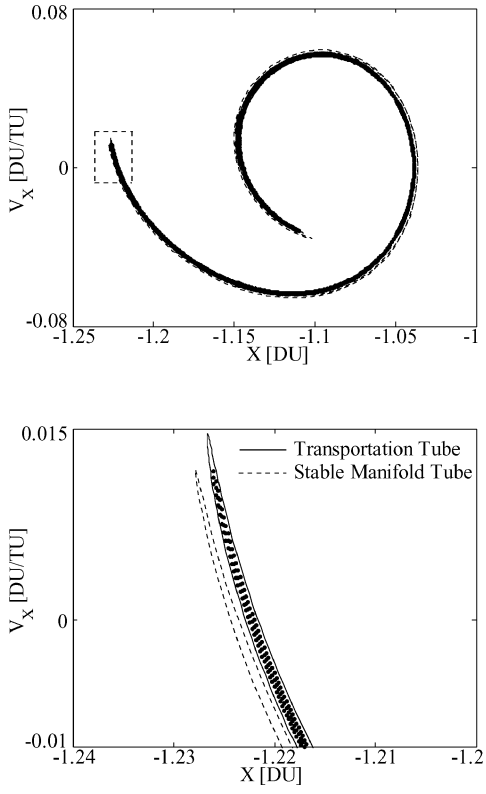

Fig. 14 Evaluation of the augmented search procedure in the CR6BPS.

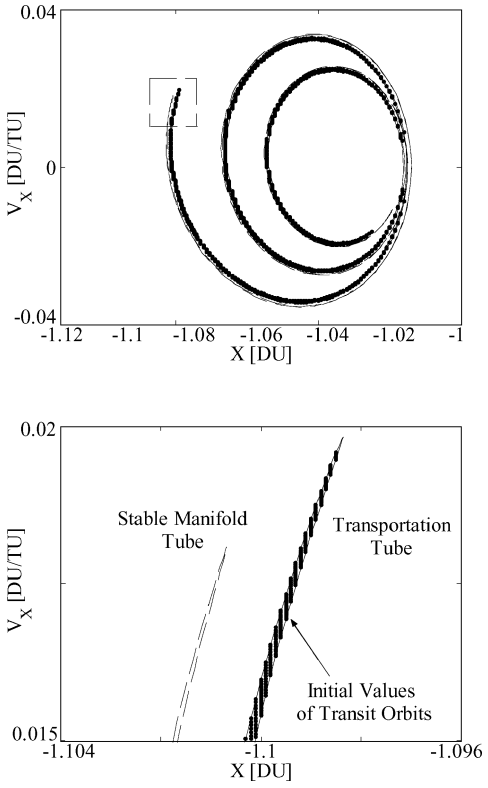

Fig. 15 Evaluation of the augmented search procedure in the CR4BP (sun–Earth/moon system with Jupiter).

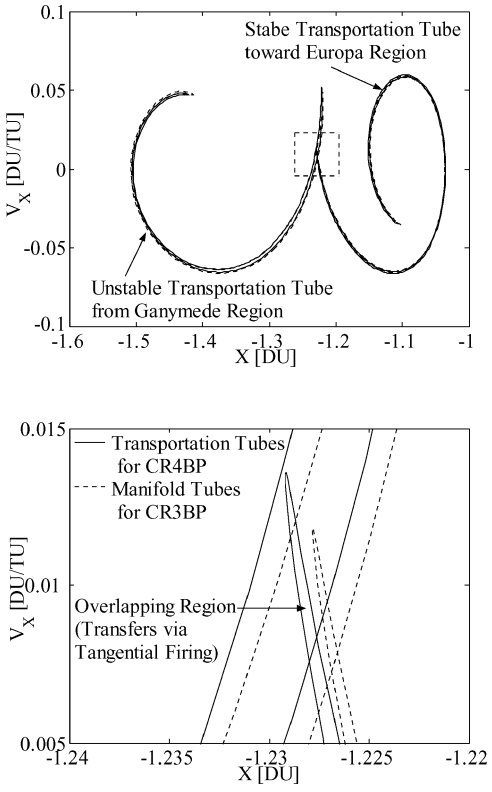

Fig. 16 Two transportation tubes in the CR4BP.[17]

Intersection of Transportation Tubes in Configuration Space

Although only the stable exterior transportation tube is focused for the numerical evaluation, bundles of transit orbits can also be found inside the other transportation tubes through the procedure in the preceding steps. Note that the set of identified transit orbits are already solutions of the dynamical model including perturbations. Thus, solution orbits in the inertial frame are immediately obtained by transforming the identified states to the inertial frame coordinates.

In the inertial frame, any celestial body orbiting around the larger primary is trailing unstable and stable transportation tubes. If two different types of transportation tubes intersect in the configuration space, it is possible for the spacecraft to jump up from one transportation tube to another by firing its thrusters. A direct application of the search procedure is the design of planar impulsive transfers between two circular and two elliptic orbits under perturbations of other bodies. Figure 16 shows an example of the intersection between unstable and stable transportation tubes in the configuration space, found in the planar Jupiter/Europa/Ganymede CR4BP system. A full description of the process of finding orbit transfers via transportation tube jumping is found in Ref. 17.

Transit-Orbit Search in the Elliptical Restricted Four-Body Problem

The wide applicability of the developed search procedure is further supported by a successful determination of a transit orbit bundle under another type of perturbation sources. By formulating the elliptical restricted four-body problem (ER4BP) as a perturbed CR3BP, the transit orbit bundle can also be identified systematically. We use the same planetary system, Jupiter–Europa elliptic three-body system with the perturbing body, Ganymede, for the numerical simulation example.

Planar Elliptic Restricted Four-Body Problem

The configuration of this model is illustrated in Fig. 17. A larger celestial body M_1, and two smaller bodies M_2 and M_3, in the same orbital plane constitute the gravitational field of this model. The motion of the spacecraft is modeled under the assumption that two

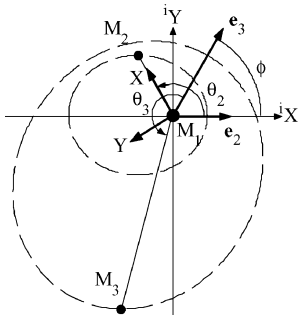

Fig. 17 Geometry of planer elliptic restricted four-body problem.

smaller bodies are on elliptical orbits with the focus at the larger body and with the different eccentricity vectors $\boldsymbol{e}_2$ and $\boldsymbol{e}_3$. In this model, the origin of the inertial frame is attached at the body M_1, the positive ${}^iX$ axis coincides with the eccentricity vector $\boldsymbol{e}_2$, and the ${}^iY$ axis is on the orbital plane. The true anomalies for the smaller bodies are represented by θ_2 and θ_3 in the figure.

After deriving the equations of motion in the inertial frame and transforming its coordinate system to the rotating frame centered at M_1 and rotating with M_2, another coordinate transformation, namely, pulsating coordinates,[27]

$$X = D_2 x, \qquad Y = D_2 y \tag{4}$$

is applied. Note that D_j denotes the distance from the larger body M_1 to the body M_j. As a result, the ER4BP model takes the form

$$x'' - 2y' = u_x^* + \varepsilon(\theta_2) u_x^*, \qquad y'' + 2x' = u_y^* + \varepsilon(\theta_2) u_y^* \tag{5}$$

where

$$u^* = \frac{\eta_1}{r_1} + \frac{\eta_2}{r_2} + \frac{\eta_3}{r_3} + \frac{1}{2}(x^2 + y^2), \qquad \eta_j = \frac{M_j}{M_1 + M_2}$$

$$\varepsilon(\theta_2) = \frac{-e_2 \cos\theta_2}{1 + e_2 \cos\theta_2}$$

$$r_1 = (x^2 + y^2)^{\frac{1}{2}}, \qquad r_2 = [(x-1)^2 + y^2]^{\frac{1}{2}}$$

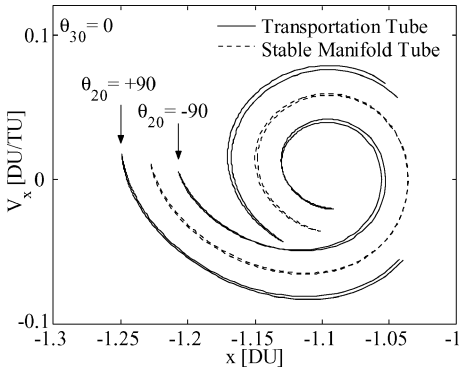

Fig. 18 Comparison between transportation and manifold tube cuts.

$$r_3 = \left\{ \left[x\cos\theta_2 - y\sin\theta_2 - \frac{D_3}{D_2}\cos(\theta_3+\phi) \right]^2 + \left[x\sin\theta_2 + y\cos\theta_2 - \frac{D_3}{D_2}\sin(\theta_3+\phi) \right]^2 \right\}^{\frac{1}{2}}$$

The prime indicates the derivative with respect to the true anomaly of the body M_2; u^* is the effective potential function in the transformed coordinates; the subscripts x and y, attached to u^*, stand for the partial derivatives with respect to x and y, respectively, and η_j for $j = 1, 2, 3$ are the normalized mass parameters. In each numerical integration time step, a root-finding iteration such as the Newton method is required to determine true anomalies θ_2 and θ_3.

The expression in Eq. (5) is very similar to the CR3BP model in Eq. (1) except for a few additional terms. These terms can be viewed as perturbations. We can expect that the phase space structure of the ER4BP in the transformed coordinates be dominated by the manifold structure similar to the CR3BP. Note that three celestial bodies M_1, M_2, and M_3 correspond to Jupiter, Europa, and Ganymede, respectively. In the subsequent numerical simulation, $e_2 = 0.009$, $e_3 = 0.002$, and $\phi = 165.2$ deg (calculated from the ephemeris data on 1 January 2003) are used for the eccentricities of two moons and the angle between the eccentricity vectors.

Transportation Tubes in ER4BP

In Fig. 18, two cuts of the transportation tubes on the Poincaré section at $\theta = 180$ deg are presented. The second-body Europa and the perturbing-body Ganymede are initially located at $\theta_{20} = \pm 90$ deg and $\theta_{30} = 0$ deg, respectively. Compared with the transportation tube cuts seen in Figs. 12 and 14, the perturbation resulting from the pulsating coordinate formulation can drastically influence the size and the location of the transportation tube in this example.

Note that the right-hand portion of the transportation tube cut for $\theta_{20} = +90$ deg cannot be obtained because of the rapid expanding feature of chaotic dynamics. Although it is desirable to develop an alternative algorithm for a portion behaving in such a chaotic manner, we focus our search of transit orbits bundle on the other parts of the tube cut.

Transit-Orbit Search in the ER4BP

Similar to the preceding cases, the Jacobi value in Eq. (2) is computed along the transportation tube cut for $\theta_{20} = +90$ deg, and the adjusted Jacobi value is obtained by simply averaging the upper and the lower values. A number of initial states on the Poincaré section are selected by the procedure in the preceding steps, and the ER4BP is numerically integrated from these initial values. Figure 19 summarizes the results of the numerical simulations. Each initial value of a transit orbit is represented by a black dot. The transportation tube successfully enwraps the bundle of the transit orbits except for the right side. In this simulation, the transit-orbit distribution varies largely from the original locations. The magnitude of the variation depends on a number of factors, including the method of problem formulations (pulsating coordinates here). The search procedure in the preceding steps can still find transit orbits even in the case where

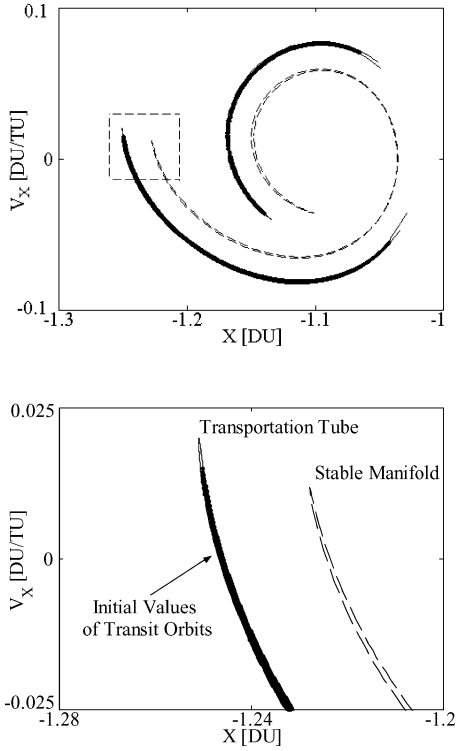

Fig. 19 Evaluation of the augmented search procedure in the ER4BP.

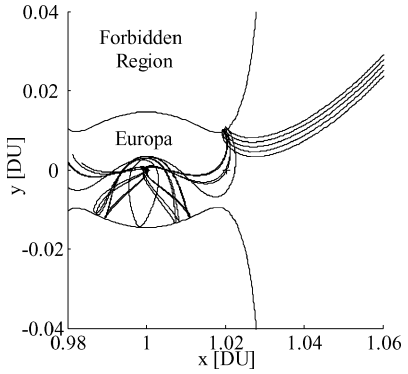

Fig. 20a Transit orbits in the ER4BP.

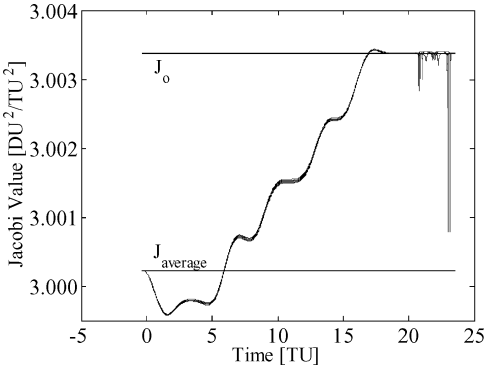

Fig. 20b Jacobi values along solution orbits.

the CR3BP system is strongly influenced by perturbations, once the transportation tube is identified.

The results of Figs. 18 and 19 also show a limitation of the presented procedure. As seen in the figures, there might exist a portion, where the transportation tube cannot be obtained, depending on initial configuration of celestial bodies and location of the Poincaré section. For the ER4BP systems with other eccentricity, such an unobtainable part can typically appear. If an unobtainable part exists,

it is commonly located in the side corresponding to the direction of the first primary (the right-hand side, that is, the direction to Jupiter, in Fig. 19). These parts, where the tube cut cannot be computed by the steps of the procedure in the section on transportation tubes in perturbed CR3BP, become sizable for larger eccentricity, such as 0.05. In that case, the presented procedure can be applied only for the successfully identified part of transportation tube cut.

Figure 20 shows example solution trajectories starting from $x = -1.25$ DU and $y = 0$ DU with several velocity magnitudes and the Jacobi values along these solution orbits. The rapid fluctuation appearing around $t = 22$ TU in Fig. 20b is caused by the extremely close distance to the primary point mass. In these example trajectories, most of the orbits collide with Europa. Recall that the transit orbits are already solutions of the ER4BP. We can immediately obtain transit trajectories consistent with the inertial frame model through the coordinate transformation.

Conclusions

In this paper, we examined the effect of perturbing forces on the orbital structure of the planar CR3BP phase space through the numerical simulations. Based on the knowledge gained, we developed a new search procedure, which enables one to find a set of trajectories involving the transition of the region (and therefore an encounter with the second body) for the planar CR3BP under perturbations. The validity of the procedure is evaluated by simulating the circular restricted problem of six bodies with the sun as well as the elliptic restricted problem of four bodies. From the results of these simulations, we conclude that the presented method is an effective means to locate transit orbit bundles in the planar CR3BP system with perturbations.

The main advantage in the design method is its wide applicability. The idea used in this paper is applicable to various dynamical systems viewed as a planar CR3BP with perturbations. Another notable feature is that the search procedure can directly find a bundle of transit trajectories consistent with the full-body dynamical system. However, the presented method is limited only on planar CR3BP models. For future work, the procedure will be extended so that we can directly find transit orbits in the spatial CR3BP with perturbations. We also consider the further inclusion of other perturbation sources, such as the oblateness of celestial bodies and the solar radiation pressure.

Acknowledgments

This paper is based on a conference paper presented at the 13th Space Flight Mechanics Meeting, Ponce, Puerto Rico, and was selected to receive a John V. Breakwell Student Travel Award. The authors express their gratitude to the Breakwell award subcommittee for the award and Martin W. Lo from the Jet Propulsion Laboratory for the early discussions on this topic.

References

[1]Barden, B. T., "Using Stable Manifolds to Generate Transfers in the Circular Restricted Problem of Three Bodies," M.S. Thesis, School of Aeronautics and Astronautics, Purdue Univ., West Lafayette, IN, Dec. 1994.

[2]Gómez, G., and Masdemont, J., "Some Zero Cost Transfers Between Libration Point Orbits," American Astronautical Society, Paper 00-177, Jan. 2000.

[3]Howell, K. C., Barden, B. T., and Lo, M., "Application of Dynamical Systems Theory to Trajectory Design for a Libration Point Mission," *Journal of the Astronautical Sciences*, Vol. 45, No. 2, 1997, pp. 161–178.

[4]Lo, M. W., Williams, B. G., Bollman, W. E., Han, D., Hahn, Y., Bell, J. L., Hirst, E. A., Corwin, R. A., Hong, P. E., Howell, K. C., Barden, B., and Wilson, R., "Genesis Mission Design," *Journal of the Astronautical Sciences*, Vol. 49, No. 1, 2001, pp. 169–184.

[5]Wilson, R. S., and Williams, K. E., "Genesis Trajectory and Maneuver Design Strategies During Early Flight," American Astronautical Society, Paper 03-202, Feb. 2003.

[6]Belbruno, E. A., and Miller, J. K., "Sun-Perturbed Earth-to-Moon Transfers with Ballistic Capture," *Journal of Guidance, Control, and Dynamics*, Vol. 16, No. 4, 1993, pp. 770–775.

[7]Koon, W. S., Lo, M. W., Marsden, J. E., and Ross, S. D., "Low Energy Transfer to the Moon," *Celestial Mechanics and Dynamical Astronomy*, Vol. 81, No. 1–2, 2001, pp. 63–73.

[8]Koon, W. S., Lo, M. W., Marsden, J. E., and Ross, S. D., "Constructing a Low Energy Transfer Between Jovian Moons," *Contemporary Mathematics*, Vol. 292, American Mathematical Society, Providence, RI, 2002, pp. 129–145.

[9]Villac, B. F., and Scheeres, D. J., "Escaping Trajectories in the Hill Three-Body Problem and Applications," *Journal of Guidance, Control, and Dynamics*, Vol. 26, No. 2, 2003, pp. 224–232.

[10]Howell, K. C., Marchand, B. G., and Lo, M. W., "Temporary Satellite Capture of Short-Period Jupiter Family Comets from the Perspective of Dynamical Systems," *Journal of the Astronautical Science*, Vol. 49, No. 4, 2001, pp. 539–557.

[11]Koon, W. S., Lo, M. W., Marsden, J. E., and Ross, S. D., "Heteroclinic Connections Between Periodic Orbits and Resonance Transitions in Celestial Mechanics," *Chaos*, Vol. 10, No. 2, 2000, pp. 427–469.

[12]Conley, C., "Low Energy Transit Orbits in the Restricted Three-Body Problem," *SIAM Journal on Applied Mathematics*, Vol. 16, No. 4, 1968, pp. 732–746.

[13]McGehee, R. P., "Some Homoclinic Orbits for the Restricted Three-Body Problem," Ph.D. Dissertation, Dept. of Mathematics, Univ. of Wisconsin, Madison, 1969.

[14]Llibre, J., Martinez, R., and Simó, C., "Transversality of the Invariant Manifolds Associated to the Lyapunov Family of Periodic Orbits Near L2 in the Restricted Three-Body Problem," *Journal of Differential Equations*, Vol. 58, No. 1, 1985, pp. 104–156.

[15]Lo, M. W., and Ross, S. D., "The Lunar $L1$ Gateway: Portal to the Stars and Beyond," AIAA Paper 2001-4768, Aug. 2001.

[16]Lo, M. W., and Ross, S. D., "Low Energy Interplanetary Transfers Using the Invariant Manifolds of $L1$, $L2$ and Halo Orbits," American Astronautical Society, Paper 98-136, Feb. 1998.

[17]Yamato, H., and Spencer, D. B., "Orbit Transfer via Tube Jumping in Restricted Problems of Four Bodies," *Journal of Spacecraft and Rockets* (to be published).

[18]Szebehely, V. G., *Theory of Orbits: The Restricted Problem of Three Bodies*, Academic Press, New York, 1967.

[19]Dunham, D. W., and Muhonen, D. P., "Tables of Libration-Point Parameters for Selected Solar System Objects," *Journal of the Astronautical Sciences*, Vol. 49, No. 1, 2001, pp. 197–217.

[20]Howell, K. C., "Families of Orbits in the Vicinity of the Collinear Libration Points," *Journal of the Astronautical Sciences*, Vol. 49, No. 1, 2001, pp. 107–125.

[21]Wiggins, S., *Introduction to Applied Nonlinear Dynamical Systems and Chaos*, Springer-Verlag, New York, 1990, pp. 6–152.

[22]Perko, L., *Differential Equations and Dynamical Systems*, 3rd ed., Springer-Verlag, New York, 2000, pp. 181–233.

[23]Parker, T. S., and Chua, L. O., *Practical Numerical Algorithms for Chaotic Systems*, Springer-Verlag, New York, 1989, pp. 139–166.

[24]Chicone, C., *Ordinary Differential Equations with Applications*, Springer-Verlag, New York, 1999, pp. 162–176.

[25]Gómez, G., Koon, W. S., Lo, M. W., Marsden, J. E., Masdemont, J., and Ross, S. D., "Invariant Manifolds, the Spatial Three-Body Problem and Space Mission Design," American Astronautical Society, Paper 01-301, Aug. 2001.

[26]Yamato, H., "Trajectory Design Methods for Restricted Problems of Three Bodies with Perturbations," Ph.D. Dissertation, Dept. of Aerospace Engineering, Pennsylvania State Univ., University Park, Aug. 2003.

[27]Broucke, R., "Stability of Periodic Orbits in the Elliptic, Restricted Three-Body Problem," *AIAA Journal*, Vol. 7, No. 6, 1969, pp. 1003–1009.